High Modulus/Tenacity Filaments from Blends of Different Molecular Weights of Polypropylene

A. Chatterjee,[1] B. L. Deopura[2]

[1]*Department of Textile Technology, Dr. B. R. Ambedkar National Institute of Technology, Jalandhar 144011, India*
[2]*Department of Textile Technology, Indian Institute of Technology, Delhi, New Delhi 110 016, India*

Received 8 December 2003; accepted 19 July 2004
DOI 10.1002/app.21313
Published online in Wiley InterScience (www.interscience.wiley.com).

ABSTRACT: Polypropylene (PP) filaments are prepared by blending two different molecular weight components of PP. A melt-spinning process to produce filaments includes mixing of components, extrusion, and two-stage drawing, followed by a unique Gradient Drawing™ process. Blending results in highly deformable as-spun filaments with high draw ratios. For 90:10 blends of PP samples with melt flow indexes of 35 and 3, a high level of crystallinity and crystalline and amorphous orientations are obtained. A sonic modulus of 28 GPa, dynamic modulus of 20 GPa, tensile modulus of 16 GPa, and tenacity of 667 MPa are achieved. These samples are dimensionally stable up to ~100°C. All steps in the production of the filaments are continuous. © 2005 Wiley Periodicals, Inc. J Appl Polym Sci 96: 1021–1028, 2005

Key words: polypropylene; blends; modulus; strength; structure–property relations

INTRODUCTION

The addition of a small percentage of high molecular weight polypropylene (PP) in fiber-grade PP improves the properties of filaments. There are a few reports on the blending of different molecular weights of PP. Van Schooten et al.[1] reported that blending of different fractions of PP leads to lower impact resistance; however, the processing of such blends was superior to that of a PP with comparable viscosity. Lowering of the melt viscosity on blending was also reported.[2] An increase in the nucleation density and spherulitic growth rate when blending a resin with a melt flow index (MFI) of 1.7 with a 14 MFI resin was also reported.[3] There was a distinct improvement in the tenacity and modulus of the blended filament. This improvement in the mechanical property was related to increased amorphous orientation, high molecular weight segments acting as tie molecules, and a possible reduction in the crystal sizes. In another study[4] the drawing behavior of fiber-grade blends and a small percentage of plastic-grade PP was reported. According to Misra et al.,[5] an increase in polydispersity produced an increase in crystallinity, modulus, and elongation at break whereas the birefringence and tensile strength decreased. The major influence of polydispersity on the structure and properties that developed were attributed to its effect on both the elongational viscosity of the resin and the ability of the high molecular weight tails in the distribution to influence the stress-induced crystallization that occurs in the spin line. Gregor-Svetec[6] reported improved spinnability and drawability of a blend containing plastic-grade and fiber-grade PP, leading to filaments with an elastic modulus of 11 GPa and a dynamic modulus of 15.5 GPa. The improvement was attributed to the high degree of crystallinity and much higher orientation of the molecules. All these studies were limited MFRs of up to 20 and 1–2 MFR grades of PP.

In this study, an attempt was made to produce high modulus, high tenacity filaments by blending two different fiber-grade resins and ultradrawing the blend filament. Two different fiber grades of isotactic PP (35 and 3 MFIs) were blended, extruded, and subsequently drawn to a high draw ratio by Gradient Drawing™ to produce high modulus PP filaments.

EXPERIMENTAL

The PP chips with 35 and 3 MFIs were provided by M/s Reliance Industries Ltd. These two MFI grades of PP chips were tumble blended in different weight proportions and extruded in a Betol single-screw extruder. The as-spun filament was drawn through two-stage drawing in sequence at 60 and 110°C with draw ratios of X4 and X2, respectively. This was followed by gradient drawing[7] at a slow speed of about 1 m/min. In the gradient drawing process, filaments were drawn with increasing draw ratios until whitening of the filaments was visible. The draw ratio was then

Correspondence to: B. L. Deopura (deopura@textile.iitd.ernet.in).

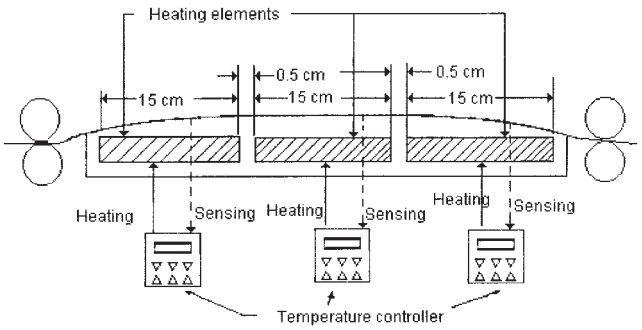

Figure 1 A schematic diagram of a gradient heater.

reduced to avoid whitening and was selected for drawing purposes. A schematic diagram of the gradient heater is shown in Figure 1. Four different temperature gradients was selected and the temperature profiles used during gradient drawing are given in Table I and Figure 2. Two-stage drawn samples are marked as D and gradient drawn samples are marked as DG1–DG4. Selected gradient drawn samples were taut heat set at 130°C for 5 min and are designated as DG4S.

Tensile properties and density

Tensile tests were carried out using a STATIMAT ME tensile tester with a gauge length of 10 cm. The strain rate was adjusted to give a time to break of 20 ± 2 s. Sonic moduli were measured in a dynamic modulus tester (PPM-5R). The fiber density was measured in a Davenport density gradient column filled with a mixture of diethylene glycol and isopropyl alcohol, which had a density range of 0.79–1.11 g/cm^3.

Thermal properties

Dynamic mechanical analysis (DMA) of the filaments was performed in a Perkin–Elmer DMA 7e. A frequency of 3 Hz was used over a temperature range of −70 to 150°C. Differential scanning calorimetry (DSC) was carried out in a Perkin–Elmer Pyris-1 with a heating rate of 10°C/min. Thermomechanical analysis (TMA) was performed in a Perkin–Elmer TMA apparatus under a load of 60 mN from 50 to 150°C with a scanning rate of 10°C/min.

Wide-angle X-ray scattering

A Philips X-ray generator was used, which was equipped with a nickel-filtered Cu Kα (0.154 nm) X-ray source and a fiber goniometer. The apparent crystalline size was determined according to the Scherer equation:

$$D_{(hkl)} = \frac{K\lambda}{\beta \cos\,\theta} \tag{1}$$

where β is the half-width of the diffraction peak (rad), K is assumed to be unity, θ is the Bragg angle, and λ is the wavelength of the X rays that were used. The values of $D_{(hkl)}$ for (110) and (040) reflections were calculated. The crystalline orientation function (f_c) was calculated using the Herman–Stein orientation function:

$$f_c = \frac{3\langle \cos^2 \phi_{c,z}\rangle - 1}{2} \tag{2}$$

where

$$\langle \cos^2 \phi_{c,z}\rangle = 1 - 1.099\langle \cos^2 \phi_{110,z}\rangle - 0.901\langle \cos^2 \phi_{040,z}\rangle \tag{3}$$

The $\cos^2\phi_{110,z}$ and $\cos^2\phi_{040,z}$ were obtained from azimuth intensity distribution measurements of (110) and (040) reflections, respectively, according to the equation[8]

$$\langle \cos^2 \phi_{hkl,z}\rangle = \frac{\int_0^{\pi/2} I(\phi)\cos^2\phi \sin\phi\, d\phi}{\int_0^{\pi/2} I(\phi) \sin\phi\, d\phi} \tag{4}$$

where $I(\phi)$ is the intensity diffracted from the (hkl) planes normal to the x-crystallographic axis. The integrals are evaluated from the intensity distribution of (110) and (040) reflections. The wide-angle X-ray diffraction (WAXD) crystallinity (χ_c) was calculated by applying the Farrow–Preston[9] method.

Amorphous orientation function

The amorphous orientation function (f_a) was calculated from the equation[10,11]

TABLE I
Temperature Profiles in Gradient Drawing

Combinations	Heater temperature		
	First (°C)	Second (°C)	Third (°C)
G1	130	130	140
G2	140	140	150
G3	140	140	160
G4	150	150	160

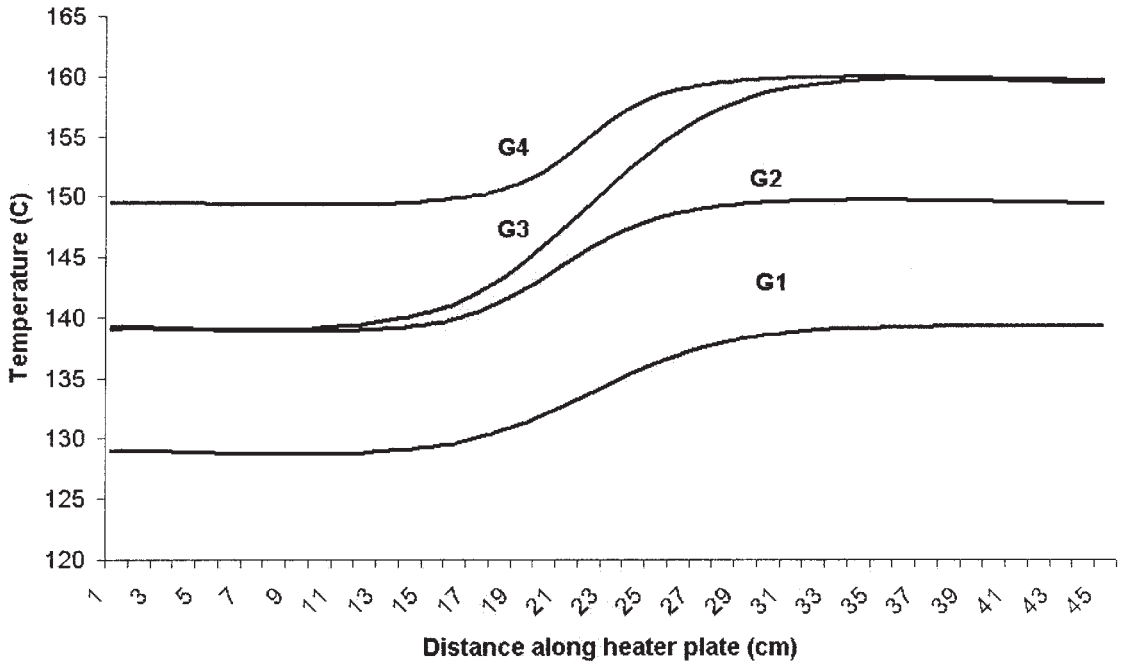

Figure 2 Temperature profiles in a gradient heater.

$$f_a = \frac{[\Delta n - \chi_{\text{X ray}} \Delta n_c f_c]}{[(1 - \chi_{\text{X ray}})\Delta n_a]} \quad (5)$$

where Δn, $\chi_{\text{X ray}}$, Δn_c, f_c, and Δn_a are the birefringence, WAXD crystallinity, intrinsic crystalline birefringence, crystalline orientation function, and intrinsic amorphous birefringence, respectively, and the Δn_c and Δn_a values are 0.033 and 0.0468, respectively.[4]

Void fraction

The volume fraction of voids (Φv) is estimated according to the method proposed by Bodaghi et al.[12] from the following equation:

$$\Phi_v = \frac{1 - \rho_s \chi_{\text{DSC}}}{\rho_c} - \frac{\rho_s(1 - \chi_{\text{DSC}})}{\rho_{am}} \quad (6)$$

where ρ_s, $\chi_{\text{X ray}}$, ρ_c, and ρ_{am} are the measured sample density, DSC crystallinity, and density of crystalline PP and the density of amorphous PP, respectively, and the ρ_c and ρ_{am} values are 0.936 and 0.857 g/cm^3, respectively.[8]

RESULTS AND DISCUSSION

The drawing conditions for the draw ratios and sonic moduli of the different samples are shown in Table II. The sonic modulus values are high in the case of the 90/10 and 50/50 blends. Thus, these two blend compositions along with the two blend components were considered for further analysis.

DSC analysis

The DSC endotherms of two different blend compositions [35/3 (90:10) and 35/3 (50:50)] along with the 35 and 3 MFI filaments are shown in Figure 3. Clear differences in the morphology of the blend filaments are noted. The 90/10 blend filament has a narrow and sharp peak compared to the 50/50 blend filament. In the 50/50 blend filament, a prominent double peak may be due to the presence of a large number of small and imperfect crystals and melting and recrystallization during DSC heating. In the 3 MFI sample there is a hump at the lower temperature side. The comparatively slower crystallization rate of 3 MFI PP leads to a broader distribution of crystal sizes. As seen from Table III, a small half-width of the melting peak indicates a high degree of crystallinity, greater perfection of the crystals, and a narrow distribution of crystal sizes in the case of the 90/10 blend filaments.

WAXD study

The results of the WAXD study of the four samples [35 MFI, 35/3 (90:10) blend, 35/3 (50:50) blend, and 3 MFI] are listed in Table IV. The WAXD study also indicates a high degree of crystallinity (74%) for the 90/10 blends. A low degree of crystallinity (42%) for the 35/3 (50:50) blend is probably due to the presence of relatively small and imperfect crystals, and this data is supported by double melting peaks in the DSC. Small and imperfect crystals may be a result of some degree of phase segregation that is attributable to

TABLE II
Draw Ratio, Sonic Modulus, and Mechanical Properties

Composition	Drawing conditions	Draw ratio	Sonic modulus (GPa)	1% Modulus (GPa)	Tenacity (MPa)	Elongation (%)
35 MFI	D	8.6	11.6	4.9	390.2	21.6
	DG1	12.6	17.3	11.8	450.1	9.4
	DG2	13.2	22.5	11.9	483.6	7.8
	DG3	13.7	23.8	12.0	485.1	7.8
	DG4	14.6	25.2	12.4	597.6	7.6
	DG4S	14.6	—	11.8	597.6	8.1
35/3 (90:10)	D	7.7	15.7	6.6	471.5	20.6
	DG1	11.9	22.5	12.3	559.0	9.1
	DG2	14.0	26.7	13.8	629.7	6.2
	DG3	14.6	28.5	14.0	632.4	6.2
	DG4	16.6	28.5	16.4	667.4	4.5
	DG4S	16.6	—	14.8	621.3	4.6
35/3 (70:30)	D	7.1	10.4	4.2	412.1	24.5
	DG1	11.2	16.5	8.5	510.3	11.8
	DG2	13.4	18.2	10.0	556.5	11.1
	DG3	14.3	22.5	10.9	560.3	9.2
	DG4	15.2	23.4	12.2	583.4	8.5
35/3 (50:50)	D	7.5	16.0	5.9	323.3	21.4
	DG1	10.1	18.2	11.4	417.9	9.1
	DG2	11.7	23.8	11.7	439.1	8.3
	DG3	12.5	25.2	13.5	439.0	7.7
	DG4	15.2	28.5	15.2	512.6	6.6
	DG4S	15.2	—	13.4	478.2	8.3
35/3 (30:70)	D	8.0	17.2	5.3	320.5	18.8
	DG1	10.0	22.3	11.4	411.2	9.5
	DG2	10.5	22.5	11.3	410.1	9.5
	DG3	12.1	22.5	12.1	462.8	8.6
	DG4	12.6	25.2	13.5	503.4	8.4
35/3 (10:90)	D	7.7	17.7	4.9	325.7	22.6
	DG1	9.6	20.0	10.6	413.1	10.5
	DG2	9.8	20.6	10.9	413.0	10.6
	DG3	11.4	22.4	11.7	459.6	8.4
	DG4	12.8	25.3	13.3	536.5	7.2
3MFI	D	7.0	14.4	4.8	410.5	23.1
	DG1	10.1	18.2	11.7	520.1	10.6
	DG2	10.3	20.2	11.2	539.0	10.2
	DG3	12.1	25.6	12.5	602.4	9.4
	DG4	12.5	27.8	13.0	615.3	8.8

widely different molecular weights. The crystal sizes as calculated for the $D_{(110)}$ and $D_{(140)}$ planes also indicate that the crystal sizes are small in the case of the 50/50 blend filament and large in the case of the 90/10 blend filament.

Amorphous and crystalline orientation function

The amorphous and crystalline orientation functions are given in Table V. All these samples exhibit a very high crystalline orientation function (f_c), but the values of the amorphous orientation functions (f_a) vary quite significantly. A maximum amorphous orientation function value of 0.88 is obtained for 35/3 (90:10) blend filaments. The 35/3 (50:50) blend filament also has an f_a value of 0.71, indicating that the blending of different molecular weights of PP helps increase the f_a values.

Void fraction

In general, the void fractions are low in all these samples, and this is attributed to the gradient drawing. Mukhopadhyay suggested[7] that, compared to being drawn on a heater plate with a single temperature, the gradient drawn samples lead to low void fractions at similar draw ratios. The void fraction of the 35/3 (50:50) blend filament is indeterminant. Void fractions largely determine the tenacity of the samples.

DMA study

The DMA curves of the 35 MFI, 35/3 (90:10), and 35/3 (50:50) blends are shown in Figures 4 and 5. The 90/10 blend has a high storage modulus of about 20 GPa followed by 16 GPa for the 50:50 blend and 10 GPa for

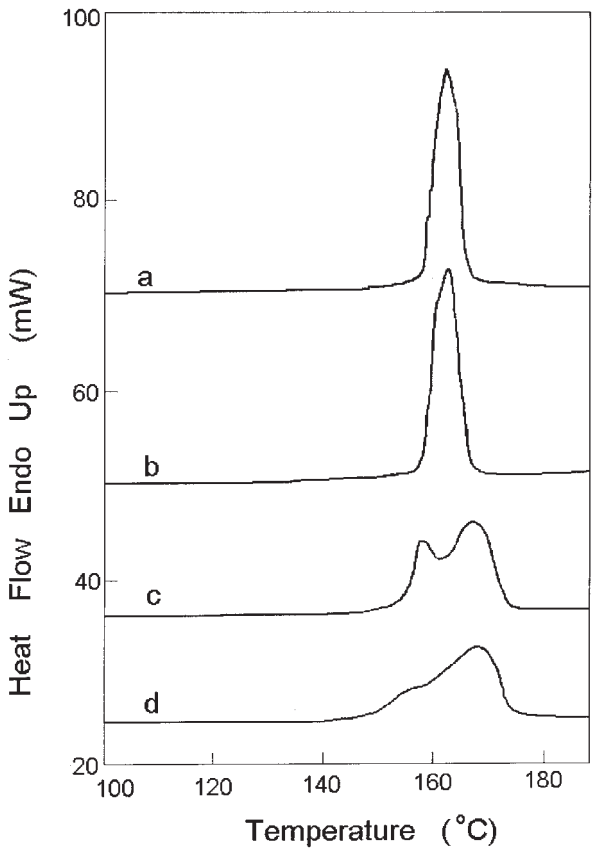

Figure 3 Melting endotherms of (a) 35 MFI, (b) 35/3 (90:10), (c) 35/3 (50:50), and (d) 3 MFI filaments.

the 35 MFI blend. There is a distinct tan δ peak for the 35 MFI filaments and a comparatively lower tan δ peak for the 50:50 blend, and the peak height is small and very broad in the 90/10 blend filament. This implies that the molecules in the 90:10 blend are in a highly oriented and ordered state and supports the high values of the crystallinity and the crystalline and amorphous orientation values.

TMA study

The TMA curves of the 35 MFI, 35/3 (90:10), and 35/3 (50:50) blends are given in Figure 6. A distinct difference in the behavior between the samples can be noticed. The 50:50 blend sample exhibits the lowest dimensional thermal stability: it is stable up to ~90°C and then it starts to shrink. Both the 90:10 and 35 MFI blends are dimensionally stable up to ~100°C. A maximum change in length takes place for the 90:10 blend followed by the 50:50 and 35 MFI filaments and in accordance with the f_a values (Table V) of the samples.

TABLE III
DSC Study for Peak Half-Width

Composition	Half-width (°C)
35 MFI	5
35/3 (90:10)	5
35/3 (50:50)	15
3 MFI	12

TABLE IV
Degree of Crystallinity and Crystal Sizes from WAXD

Composition	WAXD crystallinity (%)	$D_{(hkl)}$ at 110 (Å)	$D_{(hkl)}$ at 140 (Å)
35 MFI	66	72	88
35/3 (90:10)	74	99	113
35/3 (50:50)	42	66	79
3 MFI	64	73	86

Mechanical properties

The draw ratios, sonic moduli, and tensile properties of the samples are given in Table II.

Draw ratio

For the 90/10 blend of 35 and 3 MFIs, a maximum draw ratio of 16.6 could be achieved. It can also be seen that, with an increase in the 3 MFI component, the maximum draw ratio increases initially and then it decreases. The addition of 3 MFI PP in 35 MFI PP reduces the crystallization rate.[13] This also leads to lower as-spun crystallinity and more deformable amorphous chains, causing an increase in the draw ratios. Further addition of 3 MFI PP in the blend increases the entanglement density and reduces the draw ratios.

Sonic modulus

Maximum sonic modulus is achieved in case of the 90/10 blend filament. Comparable sonic modulus is obtained for the 50/50 blend filament and 3 MFI polymer filament. High amorphous orientation of both 90/10 and 50/50 blend filaments leads to high sonic modulus values.

TABLE V
Birefringence and Amorphous and Crystalline Orientation Functions

Composition	Δ_n	f_c	f_a
35 MFI	0.031	0.98	0.61
35/3 (90:10)	0.035	0.99	0.88
35/3 (50:50)	0.033	0.99	0.71
3 MFI	0.029	0.98	0.49

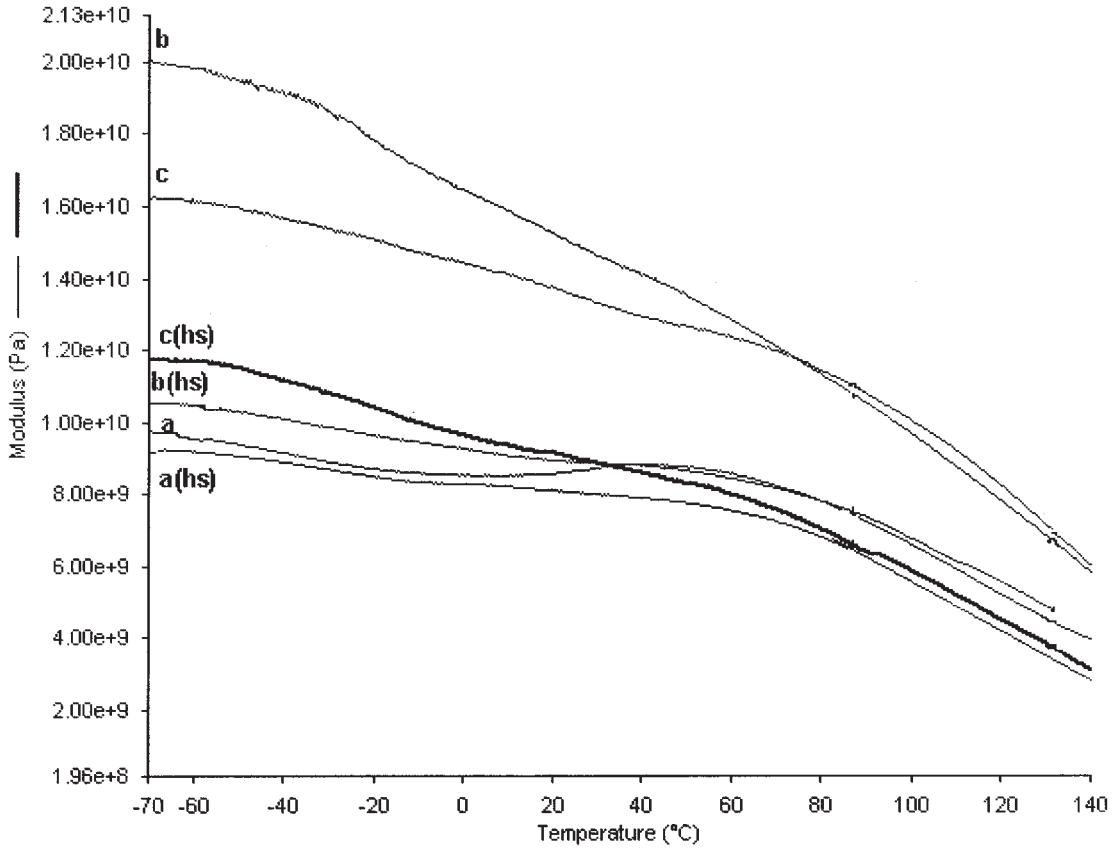

Figure 4 The storage modulus versus temperature plots of (a) 35 MFI, (b) 35/3 (90:10), and (c) 35/3 (50:50) blend filaments; hs, heat set samples.

Initial modulus and tenacity

In case of the 90/10 blend filament, a maximum initial modulus and tenacity values could be achieved followed by the 35 MFI polymer filament. Although an initial modulus value of 15.2 GPa could be achieved for the 50/50 blend filament, the tenacity value was comparatively low. The improvement in the modulus and tenacity of the 90/10 blend can be attributed to a high level of amorphous orientation, high degree of crystallinity, and narrow distribution of crystal sizes. In the 35/3 (50:50) blend filament, the initial modulus is high because of high f_a but low tenacity can be associated with small and defective crystals. The coefficient of variance (CV) of the modulus and tenacity varied from 5 to 6.5%.

Effect of heat setting

A taut heat setting was carried out for 35/3 (90:10) and 35/3 (50:50) blend filaments and the 35 MFI control sample at 130°C for 5 min. Small reductions in the initial and storage moduli of the 90:10 and 50:50 blend filaments were observed compared to the 35 MFI control sample after heat setting (Table II, Figs. 3, 4). An increased damping characteristic of the tan δ curve for the 50:50 blend followed by the 90:10 blend after heat setting is clearly seen. Stabilization through heat setting is a combined effect of crystallization and disorientation of the molecules. The results indicate that maximum disorientation has taken place in the 50:50 blend, which is expected because of its highly oriented amorphous phase and low degree of crystallinity and order. Similar behavior but with lower intensity can be seen for the 90:10 blend filament. The disorientation during heat setting leads to a change in the initial and storage moduli and tan δ values. Heat setting enhances the thermal stability of the filaments from ~100 to ~130°C as is evident from Figure 5.

CONCLUSION

Blending of 10% of 3 MFI PP with 35 MFI PP modifies the morphology of the blend, leading to a highly deformable structure. The as-spun blend filaments can be stretched to high draw ratios with improved orien-

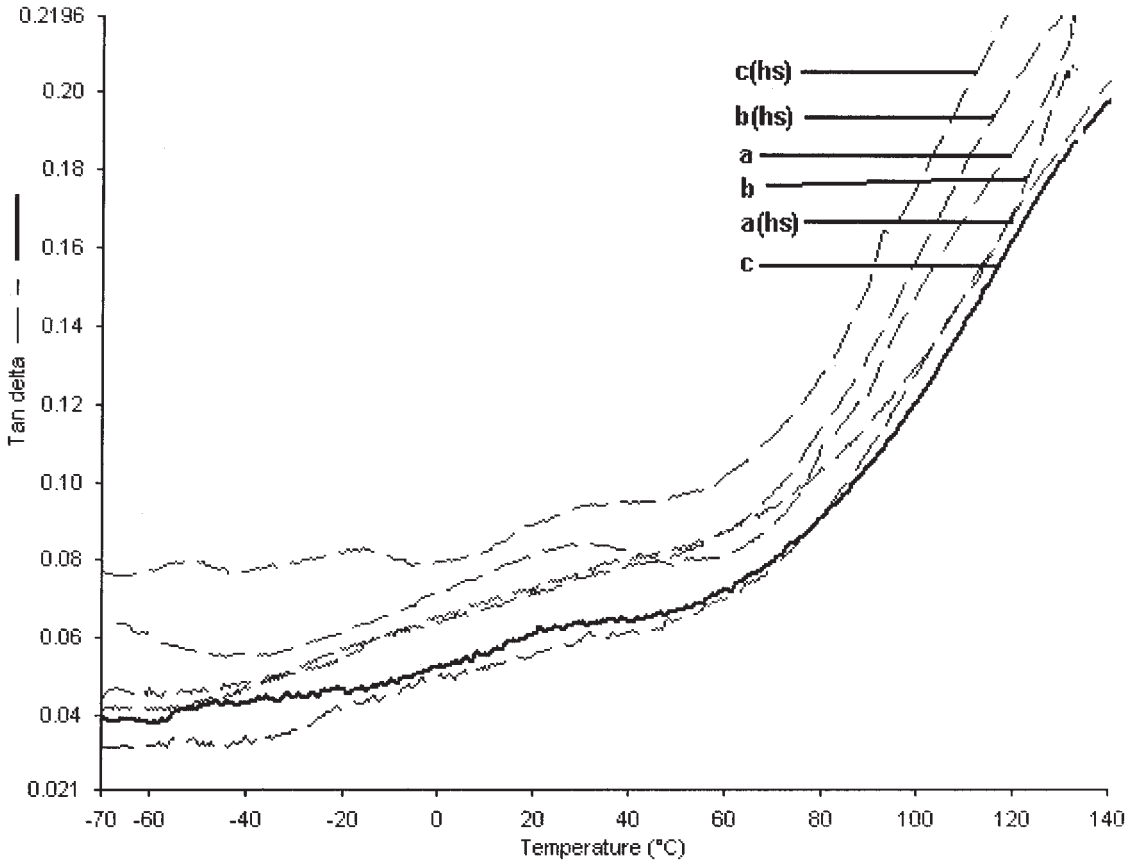

Figure 5 Tan δ versus temperature plots of (a) 35 MFI, (b) 35/3 (90:10), and (c) 35/3 (50:50) blend filaments; hs, heat set samples.

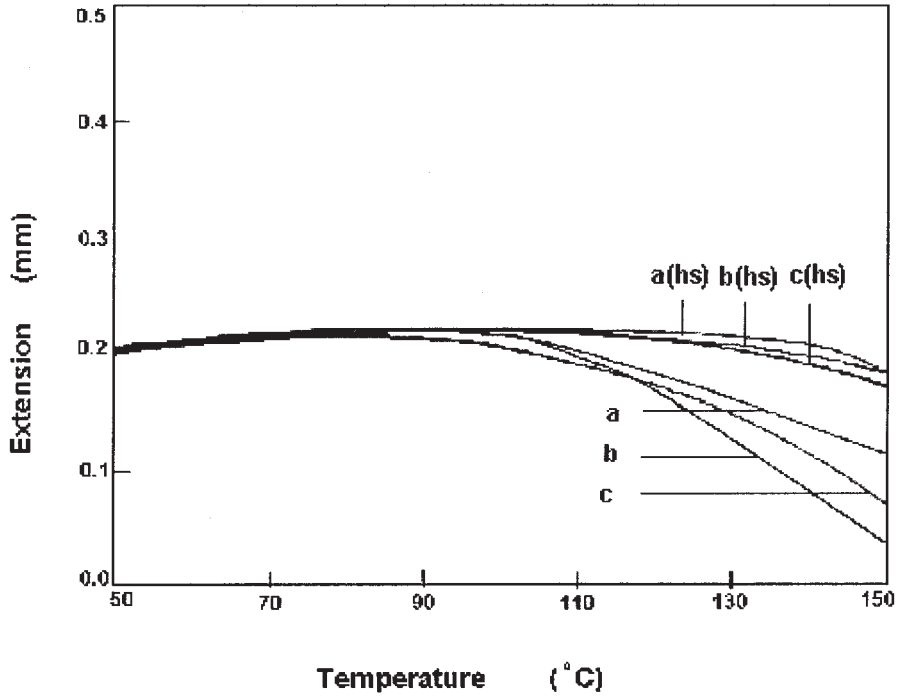

Figure 6 TMA plots of (a) 35 MFI, (b) 35/3 (90:10), and (c) 35/3 (50:50) blend filaments; hs, heat set samples.

tation. The increased orientation in turn leads to increased crystallinity, a highly oriented amorphous phase, and large crystal sizes. A combined effect of these factors leads to high modulus and tenacity values. The gradient drawing process plays a role in generating a structure having low void content and improved tenacity. The most salient feature of the whole process is development of a high modulus and high strength filament in a continuous process. This modified morphology of the 90/10 blend is stable up to ~100°C, as can be seen from the TMA curve. The thermal stability of these filaments can be enhanced by heat setting at the expense of the mechanical properties.

The authors thank Dr. S. Mahajan, Reliance Industries Limited, India, for supplying the PP chips.

References

1. Van Schooten, J.; Van Horn, H.; Borema, J. Polymer 1961, 2, 161.
2. Kamide, K.; Inamoto, Y.; Ono, K. Kobunshi Ronbunshu 1965, 22, 529.
3. Deopura, B. L.; Kadam, S. J Appl Polym Sci 1986, 31, 2145.
4. Mahajan, S. J.; Bhaumik, K.; Deopura, B. L. J Appl Polym Sci 1991, 43, 49.
5. Misra, S.; Lu, F. M.; Spruiell, J. E.; Richeson, G. C. J Appl Polym Sci 1995, 56, 1761.
6. Gregor-Svetec, D. J Appl Polym Sci 2000, 75, 1211.
7. Mukhopadhyay, S. Ph.D. Dissertation, Indian Institute of Technology, Delhi, 2004.
8. Wilchinsky, Z. W. J Appl Phys 1959, 30, 792.
9. Farrow, G.; Preston, D. Br J Appl Phys 1960, 11, 353.
10. Stein, R. S.; Norris, F. H. J Polym Sci Polym Phys 1961, 21, 381.
11. Yamamoto, Y.; Dewasawa, M.; Kinoshita, S. Sen-i Gakkaishi 1982, 38, T-10.
12. Bodaghi, H.; Spruiell, J. E.; White, J. L. In Fibrillar Structure of PP Filaments; Bodaghi, H., Ed.; Hanser: Munich, 1988; p 100.
13. Chatterjee, A.; Deopura, B. L. Fibres Polym 2003, 4, 102.